

1 **Molecular performance of Prl and Gh/Igf1 axis in the Mediterranean**
2 **meagre, *Argyrosomus regius*, acclimated to different rearing salinities**

3
4 **Khaled Mohammed-Geba^{1,3,4} (*), Antonio Astola González², Rubén Ayala Suárez²,**
5 **Asmaa Galal-Khallaf^{1,3,4}, Juan Antonio Martos-Sitcha³, Hany Mohammed Ibrahim⁵,**
6 **Gonzalo Martínez-Rodríguez³, Juan Miguel Mancera⁴.**

7
8 ¹ Genetic Engineering and Molecular Biology Division, Department of Zoology, Faculty of
9 Science, Menoufia University, Shebin El- Kom, Menoufia, Egypt.

10 ² Department of Biomedicine, Biotechnology, and Public Health, Faculty of Sciences,
11 Campus de Excelencia Internacional del Mar (CEI-MAR), University of Cadiz, 11519
12 Puerto Real, Cadiz, Spain.

13 ³ Instituto de Ciencias Marinas de Andalucía, Consejo Superior de Investigaciones
14 Científicas (ICMAN-CSIC), 11519 Puerto Real (Cádiz), Spain.

15 ⁴ Department of Biology, Faculty of Marine and Environmental Sciences, Campus de
16 Excelencia Internacional del Mar (CEI-MAR), University of Cadiz, 11519 Puerto Real,
17 Cadiz, Spain.

18 ⁵ Immunology and Parasitology Division, Department of Zoology, Faculty of Science,
19 Menoufia University, Shebin El- Kom, Menoufia, Egypt.

20

21 ***Corresponding author: Dr. Khaled Mohammed Geba.*** Genetic Engineering and
22 Molecular Biology Division, Department of Zoology, Faculty of Science, Menoufia
23 University, Shebin El- Kom, Menoufia, Egypt e-mail: khaled.mohammed@icman.csic.es.

- 24 Note: This paper follow the ZFIN Zebrafish Nomenclature Guidelines for gene and protein
25 names and symbols
26 (<https://wiki.zfin.org/display/general/ZFIN+Zebrafish+Nomenclature+Guidelines>)

27 **Abstract**

28

29 Aquaculture industry in the Mediterranean region exhibits a growing interest for the
30 Mediterranean meagre *Argyrosomus regius*. Some preliminary works showed a good
31 growth performance of the species in nearly isosmotic salinities. However, the patterns
32 of alteration of prolactin (PrI) as well as growth hormone (Gh)/insulin growth factor-1 (Igf1)
33 axis at the molecular level are not yet described in this species. Therefore, we cloned and
34 sequenced partial cDNAs for pituitary prolactin (*prl*) and growth hormone (*gh*), hepatic
35 insulin-like growth factor (*igf1*), and β -actin (*actb*). Expression patterns of these transcripts
36 were tested in juveniles of *A. regius* acclimated to four different environmental salinities:
37 i) 5 ‰ (hyposmotic); ii) 12 ‰ (isosmotic); iii) 38 ‰ (hyperosmotic; seawater control); and
38 iv) 55‰ (extremely hyperosmotic). All investigated transcripts shared high sequence
39 identities with their counterparts in other perciformes. *prl* mRNA levels showed inverse
40 pattern with increasing salinities. *gh* mRNA enhanced significantly in both 12 ‰ and 55
41 ‰ salinity groups in comparison to the control group, while *igf1* showed its maximum
42 expression levels under the nearly isosmotic environment. The results indicated clear
43 sensitivity of *prl*, *gh* and *igf1* to changes in environmental salinity, which can possibly
44 control the euryhalinity capacity of this species.

45

46 **Key words:** *actb*, *Argyrosomus regius*, *euryhaline*, *gh*, *igf1*, *prl*, *qPCR*, *salinity*.

47

48 **1- Introduction**

49

50 The Mediterranean meagre, *Argyrosmus regius*, belongs to the family Sciaenidae
51 that consists of 282 species, contributing 20 % to the world aquaculture industry. It is the
52 second globally identified group of economically important aquaculture species after the
53 groupers (family Serranidae) (Cárdenas 2010). In its normal habitats, *A. regius* is well
54 known as a species with good euryhaline capability, performing spring-summer spawning
55 migration of adults for reproduction in estuaries (brackish waters), and then getting back
56 in autumn-winter to deep waters. Juveniles remain in estuaries as nursery beds for the
57 whole summer season. They migrate later to coastal waters at the end of the summer
58 (FAO 2005-2015). The environment of this species is then dynamically-changing, moving
59 between seawater and brackish waters. These migrations should be aided by the
60 presence of an osmoregulatory system with a reasonable degree of preparedness for
61 coping with such varying ecological niches, as in other euryhaline perciformes that exhibit
62 similar migratory life pattern from the estuaries to the open seawater and vice versa (e.g.,
63 see Dean and Woo 2004; Mancera and McCormick 2007).

64 *A. regius* hatchery production started in 1996 in the south of France. Since then,
65 the hatchery production of this species has been slowly extending in the area (FAO 2015).
66 Due to its rapid growth rate, especially in the isosmotic salinities at 7-18 psu (Muñoz et
67 al. 2008), easiness in processing, low fat content and somewhat rigid texture, it gained
68 good popularity for both aquaculture producers and consumers (Monfort 2010). This
69 species has been cultured in cages and earthen ponds in both brackish water and

70 seawater conditions (Jiménez et al. 2005; El-Shebly and El-Kady 2007; Vargas-Chacoff
71 et al. 2014).

72 To our knowledge, there is no information on the endocrine control of the
73 euryhalinity on *A. regius*. Several key hormones are identified for the major roles they
74 perform in triggering the fish species acclimation to different environmental salinities,
75 mainly the hypophyseal prolactin (Prl) and growth hormone (Gh), as well as the hepatic
76 insulin-like growth factor type 1 (Igf1) (Takei and McCormick 2013). Prl is well-known as
77 a freshwater-adapting hormone. Its hyperosmoregulatory role aids the tissues to reduce
78 their general permeability, ion loss under highly ion-deficient environments, and
79 regulation of essential enzymes, channels and transporters that regulate ions passage
80 (Sakamoto and McCormick 2006; Mancera and McCormick 2007; Whittamore 2012;
81 Breves et al. 2014). These processes seem to be highly conserved on very
82 phylogenetically different euryhaline species. Gh and Igf1 roles in teleost fish
83 osmoregulation seem to be more established and understood in salmonid rather than
84 non-salmonid fishes. In salmonids, Gh/Igf1 axis exhibits plasma-hypoosmoregulatory
85 actions (Sakamoto et al. 1990; Sakamoto and McCormick 2006), increasing opercular
86 chloride cell numbers, gill Na^+, K^+ -ATPase activity and mRNA expression of
87 Na^+, K^+ -ATPase subunits, as well as salinity tolerance when administered (McCormick
88 1995, 2001). However, in non-salmonid fishes, this role is still controversial due to the
89 contradictory results obtained among different teleosts (Mancera and McCormick 1998).
90 For this reason, more research on both euryhaline and stenohaline species to determine
91 the widespread osmoregulatory actions of the Gh/Igf1 axis is required (Sakamoto and
92 McCormick 2006; Mancera and McCormick 2007; Mohammed-Geba et al. 2015).

93 This study aimed to investigate the osmoregulatory sensitivity of P_{rl} and Gh/Igf1
94 axis in *A. regius* juveniles under different environmental salinities (5, 12, 38 and 55 ‰).
95 In order to do so, partial cDNAs from *prl*, *gh* and *igf1*, together with a reference gene (β -
96 actin, *actb*), were obtained by polymerase chain reaction (PCR), cloned and sequenced.
97 The obtained gene sequences were phylogenetically analyzed to infer some common
98 pattern of expression of such transcripts in different environmental salinities among
99 similar fish species to *A. regius*, especially the ones with estuarine life stages. The
100 expression patterns of *prl*, *gh* and *igf1* mRNAs were assessed in individuals acclimated
101 to different environmental salinities using semi-quantitative real time PCR (qPCR). The
102 results are discussed in relation to the good euryhaline capacity of this species.

103

104 **2. Materials and Methods**

105

106 *2.1. Animals and experimental protocol*

107

108 Juveniles of *A. regius* (n= 32, 150-180 g body mass) were provided by IFAPA
109 Centro “El Toruño” (El Puerto de Santa María, Cádiz, Spain) and transferred to the wet
110 laboratories in the Faculty of Marine and Environmental Sciences (Puerto Real, Cádiz),
111 where they were acclimated during 7 days to 38 ‰ salinity and 21-22 °C temperature.
112 After this time, 8 animals (4 per tank) were transferred to two tanks equilibrated at 5 ‰
113 (140 mOsm kg⁻¹ H₂O), 12 ‰ (364 mOsm kg⁻¹ H₂O), 38‰ (control, 1049 mOsm kg⁻¹ H₂O)
114 and 55 ‰ (1546 mOsm kg⁻¹ H₂O). The experimental salinities were achieved by mixing
115 seawater (SW) with dechlorinated tap water (until reaching 5 ‰ and 12 ‰ salinities) or
116 with natural marine salt (Salina de la Tapa, El Puerto de Santa María, Cádiz, Spain) until
117 reaching 55 ‰ salinity. Each tank was maintained in a closed recirculating water system,
118 and a 20 % of the water was replaced every two days. To ensure optimal water conditions
119 water quality criteria (hardness, and levels of O₂, CO₂, H₂S, NO₂⁻, NO₃⁻, NH₄⁺, Ca²⁺, Cl⁻
120 and suspended solids) were monitored and no major changes were observed during the
121 experiment or between salinity treatments. Water salinity was checked daily and, when
122 necessary, adjusted to the nominal salinity by regulation of the flux of dechlorinated tap
123 water or SW. Fish were fed a daily ration of 1 % of their body mass with commercial
124 pellets (Dibaq-Dibroteg S.A., Segovia, Spain). Every morning before feeding, rearing
125 tanks were checked and no food was left. No mortality was observed during the
126 acclimation period. Fish were fasted for 1 day before sampling. After 14 days of

127 acclimation, fish were netted, anesthetized with 2 mL L⁻¹ of 2-phenoxyethanol (Sigma-
128 Aldrich, Madrid, Spain), weighed, heads separated from trunks, and organs sampled. The
129 entire pituitary gland and biopsies from the liver of each animal were immediately
130 preserved in 5-10 volumes (w/v) of RNA^{later}® (Ambion-LifeTechnologies, Madrid, Spain),
131 kept overnight at 4 °C and then transferred to -20 °C until further analysis. All experimental
132 procedures complied with the Guidelines of the European Union (2010/63/UE) and the
133 Spanish legislation (RD 1201/2005 and law 32/2007) for the use of laboratory animals.

134

135 2.2. Cloning of *A. regius prl*, *gh*, *igf1* and *actb* partial cDNAs

136

137 Gene-specific or degenerate primers for *prl*, *gh*, *igf1* and *actb* were designed from
138 published cDNA sequences, especially from perciformes, after performing an initial
139 alignment of mRNA sequences (GenBank accession numbers or NCBI Reference
140 Sequences are shown between parenthesis) using ClustalX2.1. *prl* sequences used were
141 those of *Oreochromis mossambicus* (KC702508), *Acanthopagrus schlegelii* (EU165342),
142 and *Perca flavescens* (AY332491). For *gh*, sequences used were those of *Nibeia coibor*
143 (FJ375311), *Pseudosciaena crocea* (AF231941), *Rhabdosargus sarba* (AY553207),
144 *Sparus aurata* (U01301), *Pagrus major* (X06962), *Sciaenops ocellatus* (AF063834), and
145 *Lepomis cyanellus* (AY530822). For *igf1*, the sequences aligned for primer design were
146 those from *S. aurata igf1* (total, EF563837; isoform a, Y996779; isoform b, EF688015;
147 isoform c, EF688016), *S. ocellatus* (total, GU175982; isoform ea2, GQ443298; isoform
148 ea3, GQ443299; isoform ea4, GQ443297), *Umbrina cirrosa* (AY941254), *Larimichthys*
149 *crocea* (JN565945), *Perca fluviatilis* (AJ586908), and *P. flavescens igf1b* (AY332492).

150 For *actb*, the aligned sequences were from *Danio rerio* (NM 131031), *S. aurata* (X89920),
151 *P. fluviatilis* (EU664997), *P. flavescens* (AY332493), and *L. crocea* (GU584189).
152 Sequences of degenerate and conserved cloning primers are shown in Table 1. All
153 primers used were purified by desalting and purchased from biomers.net (Germany). All
154 kits were used according to manufacturer's instructions; otherwise any modification will
155 be mentioned.

156 Total RNA was extracted with the NucleoSpin® RNA XS kit and the NucleoSpin®
157 RNA II kit (Macherey-Nagel, Düren, Germany), using single pituitary glands and liver
158 biopsies, respectively. Each organ was homogenized with an IKA® Ultra-Turrax®T8 (IKA-
159 Werke, Staufen im Breisgau, Germany), and including the on-column DNA digestion
160 using the RNase-free DNase provided with the kit. RNA quality was checked in the
161 Bioanalyzer 2100 system with the RNA 6000 Pico kit for pituitary and RNA 6000 Nano kit
162 for liver (Agilent Technologies, Life Sciences, Santa Clara, California). RNA quantity was
163 measured spectrophotometrically at 260 nm with a BioPhotometer Plus (Eppendorf,
164 Hamburg, Germany). cDNA synthesis proceeded with samples with a RNA integrity
165 number (RIN) higher than 8, and total RNA concentration higher than 100 ng μL^{-1} for liver
166 or 10 ng μL^{-1} for pituitary.

167 cDNA was synthesized using SuperScript™ III Reverse Transcriptase (Invitrogen,
168 ThermoFisher Scientific, Madrid, Spain), with ~3 μg of total RNA from liver and ~100 ng
169 from pituitary. 1 U of BIOTAQ™ DNA polymerase (Bioline, Berlin, Germany) was used in
170 each PCR reaction applied for the amplification of the target genes in a total volume of
171 25 μL . The PCRs were accomplished in a Mastercycler®pro (Eppendorf, Hamburg,
172 Germany). The PCR program is shown in Table 2. Fresh PCR products were directly

173 cloned into the pCR[®]4-TOPO cloning vector (Invitrogen, ThermoFisher Scientific, Madrid,
174 Spain) and sequenced in the Unidad de Genómica of the University of Córdoba, Spain.
175 For all putative clones, forward and reverse sequencing were carried out using the
176 dideoxynucleotide chain-termination method with T3 and T7 universal primers.

177

178 *2.3. Sequence identification and phylogenetic analyses*

179

180 The obtained sequences were compared to GenBank database using Basic Local
181 Alignment Search Tool (BLAST, www.ncbi.nlm.nih.gov/blast) to confirm their identity with
182 other *prl*, *gh*, *igf1*, and *actb* cDNA sequences available there. Sequences of these genes
183 belonging to various fish species were retrieved from GenBank
184 (<http://www.ncbi.nlm.nih.gov/nucleotide/>) and aligned using ClustalW integrated into the
185 software Mega 5.0 (Tamura et al. 2011). The results were used for constructing neighbor-
186 joining trees, after determining the best nucleotide substitution model. One thousand
187 (1,000) bootstraps were applied for enhancing the reliability of the test.

188

189 *2.4. Total RNA extraction and quantitative real time polymerase chain reaction (qPCR)*

190

191 Total RNA from liver and pituitary was extracted using the same kits mentioned in
192 section 2.2, following manufacturer protocol. RNA concentration and quality were
193 assessed as previously described. All samples had RNA integrity number (RIN) values
194 >8. 250 ng from pituitaries total RNA and 500 ng from liver were separately used for cDNA
195 synthesis using qScript[™] cDNA Synthesis Kit (Quanta BioSciences, Gaithersburg,

196 Maryland, USA). Generated cDNAs were stored at -20°C for a period never exceeding
197 one month.

198 All qPCR steps were performed using PerfeCTa™ SYBR®Green FastMix™
199 (Quanta BioSciences, Gaithersburg, Maryland, USA), with cycling conditions detailed in
200 Table 2. The qPCR primers (Table 3) were designed using the software primer3
201 (<http://frodo.wi.mit.edu/primer3/>) based on the cDNA sequences described above and
202 published in GenBank (<http://www.ncbi.nlm.nih.gov/nucleotide>): *A. regius prl* (KP984534),
203 *gh* (KM402037), shared regions between *igf1_ea2* (KM402035) and *igf1_ea4*
204 (KM402036), unique zone of *igf1_ea4*, and *actb* (KM402038). All qPCR primers were
205 purified by HPLC and purchased from biomers.net (Germany).

206 qPCR reactions (10 μL), composed of 400 pg cDNA template, 5 μL PerfeCTa™
207 SYBR®Green FastMix, and 0.5 μL from each primer, were performed with the Master
208 cycler®ep Realplex² operated with Realplex 2.2 software (Eppendorf, Hamburg,
209 Germany). Reactions, ran in triplicate, were incubated at 95°C for 5 min, followed by 40
210 cycles of 95°C for 15 s and 60°C for 1 min. Non-template controls (NTCs) and non-
211 reverse transcribed RNA were used as negative controls in every experiment. A single-
212 peak melting curve was used to check for the absence of primer-dimer artifacts and non-
213 specific amplifications. *actb* was used as the internal reference gene for normalizing
214 mRNA expression data, owing its low C_T variability as we found during the qPCR runs
215 (not exceeding 0.5 C_T differences among different salinities). Relative gene quantification
216 was performed using the $\Delta\Delta C_T$ method (Livak and Schmittgen 2001).

217

218 **2.5. Statistics**

219

220 Statistical analyses were performed using one way analysis of variance (ANOVA)

221 and Tukey-HSD Post-Hoc test, after checking the normal distribution of data, using

222 Shapiro-Wilk test, and homogeneity of variance, using Leven's test, implemented in the

223 program Statgraphics Centurion XVI. Significant values were considered when $P < 0.01$.

224

225 **3- Results**

226

227 **3.1. Prolactin (prl)**

228

229 The partial *prl* cDNA fragment from *A. regius* isolated in this study was 498 base
230 pairs (bp) long (Figure 1). The nucleotide sequence showed 91 % sequence identity with
231 *S. aurata prl* (GenBank acc. no.AF060541), 90 % with *R. sarba prl* (GenBank acc. no.
232 DQ202396), and 89 % with *A. schlegelii* (GenBank acc. no. EU165342). This cDNA
233 encoded for 166 amino acids (aa). BLAST comparisons showed that our Prl aa sequence
234 belongs to the growth hormone peptides superfamily, sharing 90 % sequence identity
235 with Prl of *L. crocea* (GenBank acc. no. KKF32453), 89 % with *S. aurata* (GenBank acc.
236 no. CAD52820), and 87 % with *R. sarba* (GenBank acc. no.ABB17072). Phylogenetic
237 analysis showed the clustering of most of perciformes *prl* precursors in a single clade, in
238 which *A. regius prl* precursor was also found (Figure 2). mRNA levels of *prl* presented an
239 inverse relationship with respect to environmental salinity, with the maximum levels at the
240 lowest salinity (5 ‰) and the minimum values in the highest salinity (55 ‰) (Figure 3).

241

242 **3.2. Growth hormone (gh)**

243

244 PCR cloning for *A. regius* growth hormone cDNA resulted in an amplicon of 552
245 bp (Figure 4). Sequencing resulted in a *gh* precursor whose nucleotide sequence shared
246 97 % identity with *S. ocellatus gh* (GenBank acc. no. AF065165), 93 % with *Sineperca*
247 *kneri* (GenBank acc. no. AY155227) and *S. aurata* (GenBank acc. no. U01301), and 90

248 % with *Epinephelus coioides* (GenBank acc. no. AY038606). This nucleotide sequence
249 encoded for 184 aa, covering most of the *gh* ORF, as noted upon comparing the primary
250 protein sequence with other Gh protein sequences published in the GenBank database.
251 This comparison showed that our Gh protein sequence shared 98 % identity with *N. coibor*
252 (GenBank acc. no. ACI95760), *S. ocellatus* (UniProtKB/Swiss-Prot Q9IB11), *Siniperca*
253 *chuatsi* (GenBank acc. no. ABM67063), and 97 % with *S. aurata* (GenBank acc. no.
254 AAB19750). Our sequence was missing 8 aa from the C-terminal end and 20 aa from the
255 N-terminus, in comparison to Gh proteins full primary aa sequences in other perciforms.

256 Phylogenetic analysis for the *gh* nucleotide sequence obtained showed the
257 grouping of all *gh* nucleotide precursors of the family Sciaenidae in a single monophyletic
258 group, forming a sub-clade that is tightly related to the other subclade containing
259 members of the family of Sparidae (Figure 5).

260 *gh* mRNA enhanced in the group maintained in 12 ‰ and 55 ‰ salinities in
261 comparison to other groups. Nonetheless, the group maintained in extremely high salinity
262 presented a 3-fold increase in *gh* expression than the one maintained under seawater
263 condition (Figure 6).

264

265 3.3. *Insulin-like growth factor 1* (*igf1*)

266

267 Cloning of *igf1* cDNA by PCR resulted in two PCR products with different sizes,
268 one was 594 bp long and the other was 679 bp long (Figure 7). Both of them included the
269 full open reading frame (ORF) for the *igf1* and a part of the 3' and 5' untranslated areas
270 (UTRs). The shorter transcript shared 100 % sequence identity with the isoform *igf1_ea2*

271 from other sciaenid fish, *S. ocellatus*, but only 86 % and 83 % with isoforms *igf1_ea3* and
272 *igf1_ea4*, respectively. Hence, we termed this shorter transcript *igf1_ea2*. The longest one
273 showed 100 % nucleotide sequence identity with *S. ocellatus igf1_ea4*, 93 % with
274 *igf1_ea3*, and 87 % with *igf1_ea2*. Therefore, the longest transcript was named *igf1_ea4*.
275 This isoform is found to code for a 186 aa protein, while *igf1_ea2* coded for a 159 aa
276 protein.

277 On terms of phylogeny, both isoforms, that are always the result of alternative
278 splicing at the same *igf1* precursor, were found to belong to a monophyletic sub-clade
279 including all sciaenid *igf1* genes. The other sub-clade includes perciformes *igf1*
280 precursors (Figure 8).

281 The expression patterns for total *igf1* and for *igf1_ea4* isoform only were similar,
282 showing their maximum levels in the nearly isosmotic salinity (12 ‰) group, and the
283 minimum in individuals under hyposmotic condition (5 ‰) or seawater (38 ‰) (Figure 9).

284

285 3.4. β -actin (*actb*)

286

287 The isolated form of *A. regius actb* was 1,113 bp long (Figure 10), encoding for
288 371 aa. The nucleotide sequence showed 99 % sequence identity with *L. crocea actb*
289 (GenBank acc. no. GU584189) and *S. ocellatus* (GenBank acc. no. KC795558), 98 %
290 with *P. major* (GenBank acc. no. JN226150), and 98 % with *S. aurata* (GenBank acc. no.
291 AF384096). BLAST comparisons showed the completeness of the ORF from the 5' end,
292 but it lacked about 4 aa from the N-terminus. Primary protein structure showed 100 %
293 sequence identity with *actb* of *S. aurata* (GenBank acc. no. AEW67142), *S. ocellatus*

294 (GenBank acc. no. AGO64768), and *L. crocea* (GenBank acc. no. ACB98723). As in *prl*,
295 *gh* and both *igf1* isoforms, the cloned *actb* could be located in a sub-clade joining with the
296 large yellow croaker, *L. crocea*, the only sciaenid species other than *A. regius* which have
297 a cloned *actb* sequence (Figure 11).

298

299 **4- Discussion**

300

301 **4.1. Structure and phylogenetic results of the obtained precursors**

302

303 For the first time in the Mediterranean meagre *A. regius*, partial precursors for *prl*,
304 *gh*, *igf1*, and *actb* were cloned and sequenced. To our knowledge, the precursor of *prl*
305 provided in this study is the first to be cloned in the family Sciaenidae in general. Despite
306 being *prl* precursor in the same clade that combined *prl1* form of all vertebrates, including
307 *prl177* and *prl188* from *Oreochromis niloticus*, that were first described by Specker et al.
308 (1985), we did not isolate any further forms of *prl*. Moreover, the obtained precursor was
309 phylogenetically distant from *prl2* isoform that was previously detected in the brain and
310 the eye, but not in the pituitary, of the non-mammalian vertebrates by Huang et al. (2009).
311 However, *gh* precursor showed much more taxon-specific pattern with *gh* from all
312 representative species belonging to family Sciaenidae placed in a single cluster, Sparidae
313 in the second, Otophysi in the third, and Salmonidae in the fourth. For *igf1*, two forms
314 were identified, *igf1_ea2* and *igf1_ea4*, showing similar patterns to that of *gh*, with all *igf1*
315 forms identified in Sciaenidae belonging to the same clade. In general, there is a
316 phylogenetic ambiguity in what concerns *igf1* genomic copies, although it is commonly
317 accepted that such copies share a high degree of similarity in their coding regions
318 (Moghadam et al. 2007). Alternative splicing for *igf1* precursor was described in different
319 fish and non-fish models, but duplication in the genomic DNA of *igf1* in sciaenids or in
320 other perciformes cannot be clearly judged since the difference in these duplicate copies
321 is mainly distinctive in the 3' and 5' UTRs of *igf1* genes, not in the ORFs (Zou et al. 2009).

322 The cloned *actb* precursor clustered in a single clade with its counterparts in other fish
323 species that previously showed the least *actb* expression changes upon different
324 treatments, such like *L. crocea* and *E. coioides* (Zhang et al. 2004; Chen et al. 2015).

325

326 4.2. Regulation of hormonal transcripts by different environmental salinities

327

328 For the first time, Mediterranean meagre *A. regius prl*, *gh*, *igf1* and *actb* cDNAs
329 could be cloned, sequenced and tested, using quantitative real time PCR, under different
330 environmental salinity regimes. This study aimed directly to pursue the state expression
331 of *prolactin* and main elements in the Gh/Igf1 axis in different environmental salinities to
332 which fish are normally subjected to in their native habitats (hyposmotic, isosmotic, and
333 hyperosmotic) (Cardenas 2010, FAO 2005-2015). This study can aid future works that
334 aim to assess growth and survival of this species under different salinities. Our results
335 indicated a classical inverse response of *prl* to environmental salinity, together with about
336 2 to 4-fold upregulation for *igf1* in the nearly isosmotic salinity in comparison to seawater,
337 which may be in line with the known roles of Igf1 in stimulating salinity tolerance promoting
338 growth (Takei and McCormcik 2013).

339 Molecular endocrinological alterations due to salinity acclimation is a completely
340 dark zone in *A. regius*. However, some clues to the way Prl and the Gh/Igf1 axis response
341 to environmental salinity alterations can be obtained from similar teleost species,
342 especially the ones that succeed under different environmental salinities. *prl* inverse
343 correlation with environmental salinities is well considered as an essential adjustment
344 mechanism in many euryhaline teleost species, including *A. regius* as we found in the

345 current work. This pattern and the potent roles in inducing proper osmoregulation in
346 response to hyposmotic salinities is very conserved in many fish species, despite being
347 very phylogenetically-diverse (McCormick 2001; Sakamoto and McCormick 2006). *prl*
348 can be regulated by the changes in environmental salinity due to the osmosensitivity of
349 pituitary prolactotrophs (Manzon 2002;; Fuentes et al. 2010. Kültz, 2013). Minute changes
350 in the extracellular osmolality, together with the presence of some autocrine modulator
351 proteins like Prl₁₇₇ and Prl₁₈₈, directly triggered Prl production in the European eel, *S.*
352 *aurata*, and the tilapias (Suzuki et al. 1991; Uchida et al. 2004; Mohammed-Geba et al.
353 2015; Yamaguchi et al. 2016). Moreover, it is noteworthy to mention that both plasma Prl
354 levels and pituitary *prl* expression patterns corresponded in their upregulation in response
355 to hyposmotic salinity in different perciform species, like *O. mossambicus* and *S. aurata*
356 (Riley et al. 2003; Laiz-Carrión et al 2009; Vargas-Chacoff et al. 2009). Hence, the *prl*
357 upregulation we found in *A. regius* under low salinity can directly contribute to the species
358 survival in environments like estuaries and coastal lagoons that are known to be within
359 the native range of life of this species, as mentioned before.

360 *gh* and *igf1* expression levels enhanced under isosmotic conditions. Regarding
361 *igf1*, both primer sets, designed for the *igf1_ea4* and *igf1_ea2* shared region and for the
362 unique sequence of *igf1_ea4* mRNA, showed a 2 to 4-fold upregulation of *igf1* in the
363 nearly isosmotic salinity than in the normal seawater salinity. On the other hand, *igf1* gene
364 active transcription in relation to growth is known, signifying that the more production of
365 such hormone the better growth the organism exhibits (Wood et al. 2005). This can
366 explain the low energy expenditure and the high growth rates noted for *A. regius* when
367 reared under isosmotic salinity (Muñoz et al. 2008). *igf1* upregulation in nearly isosmotic

368 salinity and a corresponding enhanced growth and metabolism was previously reported
369 in other euryhaline perciformes experiencing isosmotic environments, such like *Sparus*
370 *sarba* and *Mylio macrocephalus* (Woo and Kelly 1995; Deane and Woo 2004, 2005). The
371 abundance of Igf1 receptors in teleost muscles contribute directly to the enhancement of
372 growth by this hormone, both *in vivo* and *in vitro* (Kwasek et al. 2015; Vélez et al. 2016).
373 Therefore, the upregulation in *A. regius igf1* under isosmotic salinity found in the current
374 study, could participate in the growth enhancement noted before in this species reared
375 under similar environments (Muñoz et al. 2008).

376 Interestingly, *gh* expression enhanced under the hyperosmotic environment
377 tested herein (55 ‰), while observed *igf1* increase was not statistically significant in the
378 same environment in comparison to normal seawater control group. This *gh* upregulation
379 agrees with the hyposmotic role of this axis in other teleost species, as mentioned before
380 in the introduction section. Gh stimulates general cell proliferation in gills, including the
381 mitochondria-rich cells (Gonzalez 2012). Despite the role of Gh in promoting acclimation
382 to hypersaline environments is almost constitutive in salmonids, non-salmonid fishes
383 exhibit contradictory Gh responses and under such salinities (Mancera and McCormick
384 1998; Deane and Woo 2009). Our results for *gh* upregulation in the hyperosmotic
385 environment agreed with what was found before in another estuarine teleost, *S. aurata*,
386 that was subjected to the same environmental salinity 55 ‰ (Mohammed-Geba et al.
387 2015). *S. aurata* is known to have very similar life pattern to that of *A. regius*, including
388 the transition between open sea and estuaries. This can suggest then a common role for
389 Gh, in the estuarine perciformes, in aiding acclimation to extremely hyperosmotic

390 environments, possibly through modifying osmotic adjustments required for fish survival
391 under such environments.

392

393 *4.3. Conclusions*

394

395 The Mediterranean meagre *A. regius* proved to be a robust fish species, tolerating
396 a wide range on environmental salinities (5-55 ‰). *A. regius prl* exhibited the classic
397 inverse response to changes in environmental salinity, indicating that in this species Prl
398 performed its conserved hyperosmoregulatory role. *igf1* peaked in the nearly-isosmotic
399 salinity, correspondent with enhanced growth in other estuarine perciformes. *gh* seemed
400 to play a role in the survival of *A. regius* individuals in the extremely hypersaline
401 environment, due to its specific upregulation in such environment, plausibly in order to
402 supply metabolic energy for acclimation under this extreme salinity. Finally, and since the
403 best growth of *A. regius* was noted in the isosmotic salinity, Prl and the Gh/Igf1 axis are
404 likely to participate in such good performance through stimulating fish acclimation to this
405 salinity.

406

407 ***Acknowledgments***

408

409 This work was carried out as a part of the Spanish-Egyptian joint project
410 AP/039755/11(Development of molecular, physiological and immunological biomarkers
411 for the detection of stress related to the Mediterranean meagre aquaculture *Argyrosomus*
412 *regius*) awarded from the Spanish agency of international cooperation (Agencia Española

413 de Cooperación Internacional, AECID) and the Egyptian Academy of Scientific Research
414 and Technology, to Juan Miguel Mancera (Universidad de Cádiz, Spain) and Khaled
415 Mohammed-Geba (Menofia University, Egypt). The authors would like to express their
416 thanks to Prof. Saber Abd El-Rahman Sakr, head of the Zoology Department, Faculty of
417 Science, Menofia University, Egypt, for his sincere help during the development of the
418 project's strategies and bureaucratic work.

419

420 **References**

- 421 Acha EM, Mianzan H, Lasta CA, Guerrero RA (1999) Estuarine spawning of the white
422 mouth croaker *Micropogonias furnieri* (Pisces: Sciaenidae), in the Río de la Plata,
423 Argentina. *Mar Fresh Res* 50(1):57-65.
- 424 Bernatzeder AK, Cowley PD, Hecht T (2010) Do juveniles of the estuarine-dependent
425 dusky kob, *Argyrosomus japonicus*, exhibit optimum growth indices at reduced
426 salinities? *Estuarine Coast Shelf Sci* 90:111-115.
- 427 Fielder DS, Bardsley W (1999) A preliminary study on the effects of salinity on growth
428 and survival of mullet *Argyrosomus japonicus* larvae and juveniles. *J World*
429 *Aquacult Soc* 30:380-387.
- 430 Bœuf G, Payan P (2001) How should salinity influence fish growth? *Comp Biochem*
431 *Physiol* 130C:411–423.
- 432 Breves JP, Seale AP, Moorman BP, Lerner DT, Moriyama S, Hopkins KD, Grau EG
433 (2014). Pituitary control of branchial NCC, NKCC and Na⁺, K⁺-ATPase α -subunit
434 gene expression in Nile tilapia, *Oreochromis niloticus*. *J Comp Physiol B*
435 184(4):513-523.
- 436 Cárdenas S (2010) Crianza de la corvina *Argyrosomus regius*. *Cuadernos de Acuicultura*
437 3:12-57. Chen S, Pu L, Xie F, Zou Z, Jiang Y, Han K, Wang Y, Zhang Z (2015).
438 Differential expression of three estrogen receptors mRNAs in tissues, growth
439 development, embryogenesis and gametogenesis from large yellow croaker,
440 *Larimichthys crocea*. *Gen Comp Endocrinol*. 216: 134-51.
- 441 Deane EE, Woo NYS (2005) Cloning and characterization of sea bream Na⁺-K⁺-ATPase
442 α and β subunit genes: *In vitro* effects of hormones on transcriptional and
443 translational expression. *Biochem Biophys Res Commun* 331:1229–1238.
- 444 Deane EE, Woo NY (2005) Upregulation of the somatotrophic axis is correlated with
445 increased G6PDH expression in Black Sea bream adapted to iso-osmotic salinity.
446 *Ann NY Acad Sci* 1040:293–296.
- 447 Deane EE, Woo NY (2009) Modulation of fish growth hormone levels by salinity,
448 temperature, pollutants and aquaculture related stress: a review. *Rev Fish Biol*
449 *Fish* 19:97-120.

450 Deane EE, Woo NYS (2004) Differential gene expression associated with euryhalinity in
451 sea bream (*Sparus sarba*). Am J Physiol 287:R1054-R1063.

452 El-Shebly AA, El-Kady MAH (2007) Preliminary observations on the pond culture of
453 meagre *Argyrosomus regius* (Asso, 1801) (Sciaenidae) in Egypt. J Fish Aquat Sci
454 2:345-352.

455 FAO 2005-2015 Cultured Aquatic Species Information Programme. *Argyrosomus regius*.
456 Cultured Aquatic Species Information Programme. Text by Stipa P; Angelini M. In:
457 FAO Fisheries and Aquaculture Department [online]. Rome. Updated 10 February
458 2005 [Cited 12 October 2015].

459 Ferreira HL, Vine NG, Griffiths CL, Kaiser H (2008) Effect of salinity on growth of juvenile
460 silver kob, *Argyrosomus inodorus* (Teleostei: Sciaenidae). African J Aquat Sci
461 33:161-165.

462 Fuentes J, Brinca L., Guerreiro PM, Power DM (2010). PRL and GH synthesis and
463 release from the sea bream (*Sparus auratus* L.) pituitary gland in vitro in response
464 to osmotic challenge. Gen Comp Endocrinol 168(1), 95-102.

465 Gonzalez, R. J. (2012). The physiology of hyper-salinity tolerance in teleost fish: a review.
466 J Comp Physiol B 182(3):321-329.

467 Huang X, Hui MN, Liu Y, Yuen DS, Zhang Y, Chan WY, Lin HR, Cheng SH, Cheng CH
468 (2009). Discovery of a novel prolactin in non-mammalian vertebrates: evolutionary
469 perspectives and its involvement in teleost retina development. PLoS One
470 4(7):e6163.

471 Jiménez MT, Pastor E, Grau A, Alconchel JI, Sánchez R, Cárdenas S (2005) Review of
472 sciaenid culture around the world, with a special focus on the meagre *Argyrosomus*
473 *regius* (Asso, 1801). Boletín Instituto Español de Oceanografía 21:169-175.

474 Kalujnaia S, McWilliam IS, Zaguinaiko VA, Feilen AL, Nicholson J, Hazon N, Cutler CP,
475 Balment RJ, Cossins AR, Hughes M, Cramb G (2007) Salinity adaptation and gene
476 profiling analysis in the European eel (*Anguilla anguilla*) using microarray
477 technology. Gen Comp Endocrinol 152:274–280.

478 Kültz, D. (2013) Osmosensing. In: McCormick S.D., Farrell A.P., Brauner C.J. Euryhaline
479 fishes Vol 32. Academic Press, New York, pp 45-68.

480 Kwasek K, Wick M, Dabrowski K (2015). Muscle Protein Characteristic and Its
481 Association with Faster Growth in Percids and Other Teleosts. In *Biology and*
482 *Culture of Percid Fishes* (pp. 339-352). Springer Netherlands.

483 Laiz-Carrión R., Fuentes J., Redruello B., Guzmán J.M., Martín del Río M.P. and Mancera
484 J.M. (2009) Expression of pituitary prolactin, growth hormone and somatolactin is
485 modified in response to different stressors (salinity, crowding and food-deprivation)
486 in gilthead sea bream *Sparus auratus* Gen. Comp. Endocrinol. 162: 293-300
487 (2009)

488 Livak KJ, Schmittgen TD (2001) Analysis of relative gene expression data using real-time
489 quantitative PCR and the $2^{-\Delta\Delta C_T}$ method. *Methods* 25:402–408

490 Lo PC, Liu SH, Chao NL, Nunoo FK, Mok HK, Chen WJ (2015) A multi-gene dataset
491 reveals a tropical New World origin and Early Miocene diversification of croakers
492 (Perciformes: Sciaenidae). *Mol Phylogenet Evol* 88:132-43.

493 Magdeldin S, Uchida K, Hirano T, GRAU EG, Abdelfattah A, Nozaki M (2007) Effects of
494 environmental salinity on somatic growth and growth hormone/insulin-like growth
495 factor-I axis in juvenile tilapia *Oreochromis mossambicus*. *Fish Sci* 73:1025-1034.

496 Mancera JM, McCormick SD (1998) Osmoregulatory actions of the GH/IGF-1 axis in non-
497 salmonid teleosts. *Comp Biochem Physiol* 121B:43-48.

498 Mancera JM, McCormick SD (2007) Role of prolactin, growth hormone, insulin-like growth
499 factor I and cortisol in teleost osmoregulation. *Fish Osmoregulation* 497-515.

500 Manzon LA. (2002). The role of prolactin in fish osmoregulation: a review. *Gen Comp*
501 *Endocrinol*, 125(2), 291-310.

502 McCormick SD (1995) Hormonal control of gill Na^+, K^+ -ATPase and chloride cell function.
503 In: Wood CM, Shuttleworth TJ (eds), *Fish Physiology*, vol. 14, Academic Press,
504 New York. Pp, 285-315.

505 McCormick SD (2001) Endocrine control of osmoregulation in teleost fish. *Am Zool* 41:
506 781-794.

507 Moghadam HK, Ferguson MM, Rexroad CE 3rd, Coulibaly I, Danzmann RG (2007).
508 Genomic organization of the IGF1, IGF2, MYF5, MYF6 and GRF/PACAP genes
509 across Salmoninae genera. *Anim Genet* 38(5):527-32.

510 Mohammed-Geba, K., Mancera, J. M., Martínez-Rodríguez, G. (2015). Acclimation to
511 different environmental salinities induces molecular endocrine changes in the
512 GH/IGF-I axis of juvenile gilthead sea bream (*Sparus aurata* L.). *J Comp Physiol*
513 *B* 185(1):87-101.

514 Monfort MC (2010) Present market situation and prospects of meagre (*Argyrosomus*
515 *regius*), as an emerging species in Mediterranean aquaculture. *Studies and*
516 *Reviews*. General Fisheries Commission for the Mediterranean. No. 89. Rome,
517 FAO. 2010. 28p.

518 Muñoz JL, Rodríguez-Rúa A, Bustillos P, et al. (2008). Crecimiento de corvina
519 *Argyrosomus regius* (Asso, 1801) en estanques de tierra a distintas salinidades.
520 IV Jornadas de Acuicultura en el Litoral Suratlántico. Nuevos retos. Cartaya,
521 Huelva, Spain.

522 Peters KM, McMichael RH (1987) Early life history of the red drum, *Sciaenops ocellatus*
523 (Pisces: Sciaenidae), in Tampa Bay, Florida. *Estuaries* 10:92-107.

524 Riley LG, Hirano T, Grau EG (2003). Effects of transfer from seawater to fresh water on
525 the growth hormone/insulin-like growth factor-I axis and prolactin in the Tilapia,
526 *Oreochromis mossambicus*. *Comp Biochem Physiol* 136B(4): 647-655.

527 Sakamoto T, McCormick SD (2006) Prolactin and growth hormone in fish osmoregulation.
528 *Gen Comp Endocrinol* 147(1):24-30.

529 Sakamoto T, McCormick SD, Hirano T (1993) Osmoregulatory actions of growth hormone
530 and its mode of action in salmonids: A review. *Fish Physiol Biochem* 11:155-64.

531 Sakamoto T., Ogasawara T., Hirano T. (1990). Growth hormone kinetics during
532 adaptation to a hyperosmotic environment in rainbow trout. *J Comp Physiol B*
533 160(1): 1-6.

534 Specker JL, King DS, Nishioka RS, Shirahata K, Yamaguchi K, Bern HA (1985) Isolation
535 and partial characterization of a pair of prolactins released in vitro by the pituitary
536 of cichlid fish, *Oreochromis mossambicus*. *Proc Natl Acad Sci USA* 82:7490–7494.

537 Schultz ET, McCormick SD (2013) Euryhalinity in an evolutionary context.. In: McCormick
538 S.D., Farrell A.P., Brauner C.J. *Euryhaline fishes* Vol 32. Academic Press, New
539 York, pp 478-533.

540 Suzuki R., Kaneko T., Hirano T. (1991). Effects of osmotic pressure on prolactin and
541 growth hormone secretion from organ-cultured eel pituitary. *J Comp Physiol B*
542 161(2):147-153.

543 Takei Y., McCormick, S.D (2013). Hormonal control of fish euryhalinity. In: [McCormick](#)
544 [S.D., Farrell A.P., Brauner C.J. Euryhaline fishes Vol 32. Academic Press, New York, pp](#)
545 [70-125.](#)

546 Tamura K, Peterson D, Peterson N, Stecher G, Nei M, Kumar S (2011) MEGA5:
547 molecular evolutionary genetics analysis using maximum likelihood, evolutionary
548 distance, and maximum parsimony methods. *Mol Biol Evol* 28:2731-2739.

549 Tang Y, Shepherd BS, Nichols AJ, Dunham R, Chen TT (2001) The influence of
550 environmental salinity on messenger RNA levels of growth hormone, prolactin, and
551 somatolactin in pituitary of the channel catfish (*Ictalurus punctatus*). *Mar*
552 *Biotechnol* 3:205–217.

553 Tiago DM, Laizé V, Cancela ML (2008) Alternatively spliced transcripts of *Sparus aurata*
554 insulin-like growth factor 1 are differentially expressed in adult tissues and during
555 early development. *Gen Comp Endocrinol* 157:107-115.

556 Uchida K., Yoshikawa-Ebesu JS, Kajimura S, Yada T, Hirano T, Grau EG (2004). In vitro
557 effects of cortisol on the release and gene expression of prolactin and growth
558 hormone in the tilapia, *Oreochromis mossambicus*. *Gen Comp Endocrinol* 135(1):
559 116-125.

560 Vargas-Chacoff L, Astola A, Arjona FJ, Del Río MM, García-Cózar F, Mancera JM,
561 Martínez-Rodríguez G (2009). Gene and protein expression for prolactin, growth
562 hormone and somatolactin in *Sparus aurata*: seasonal variations. *Comp Biochem*
563 *Physiol* 153B(1): 130-135.

564 Vargas-Chacoff L, Ruiz-Jarabo I, Pascoa I, Gonçalves O, Mancera JM (2014) Yearly
565 growth and metabolic changes in earthen pond-cultured meagre *Argyrosomus*
566 *regius*. *Scientia Marina* 78:193-202.

567 Varsamos S, Xuereb B, Commes T, Flik G, Spannings-Pierrot C (2006) Pituitary hormone
568 mRNA expression in European sea bass *Dicentrarchus labrax* in seawater and
569 following acclimation to fresh water. *J Endocrinol* 191:473-480.

570 Vélez EJ, Lutfi E, Azizi S, Perelló M, Salmerón C, Riera-Codina M, Ibarz A, Fernández-
571 Borràs J, Blasco J, Capilla E, Navarro I, Gutiérrez J (2016). Understanding fish
572 muscle growth regulation to optimize aquaculture production. *Aquaculture*
573 [doi:10.1016/j.aquaculture.2016.07.004](https://doi.org/10.1016/j.aquaculture.2016.07.004).

574 Whittamore J. M. (2012). Osmoregulation and epithelial water transport: lessons from the
575 intestine of marine teleost fish. *182(1):1-39*.

576 Woo NYS, Kelly SP (1995). Effects of salinity and nutritional status on growth and
577 metabolism of *Sparus sarba* in a closed seawater system. *Aquacult 135: 229–238*.

578 Wood AW, Duan C, Bern HA (2005). Insulin-like growth factor signaling in fish. *Int Rev*
579 *Cytolog 243, 215-285*.

580 Yamaguchi Y, Moriyama S, Lerner DT, Gordon Grau E, Seale AP (2016). Autocrine
581 positive feedback regulation of prolactin release from tilapia prolactin cells and its
582 modulation by extracellular osmolality. *Endocrinol en-2015*

583 Zhang Y1, Zhang W, Zhang L, Zhu T, Tian J, Li X, Lin H (2004). Two distinct cytochrome
584 P450 aromatases in the orange-spotted grouper (*Epinephelus coioides*): cDNA
585 cloning and differential mRNA expression. *J Steroid Biochem Mol Biol 92(1-*
586 *2):39-50*.

587 Zou S, Kamei H, Modi Z, Duan C (2009). Zebrafish IGF genes: gene duplication,
588 conservation and divergence, and novel roles in midline and notochord
589 development. *PLoS One, 4(9), e7026*.

590

591

592 **Legends to Figures**

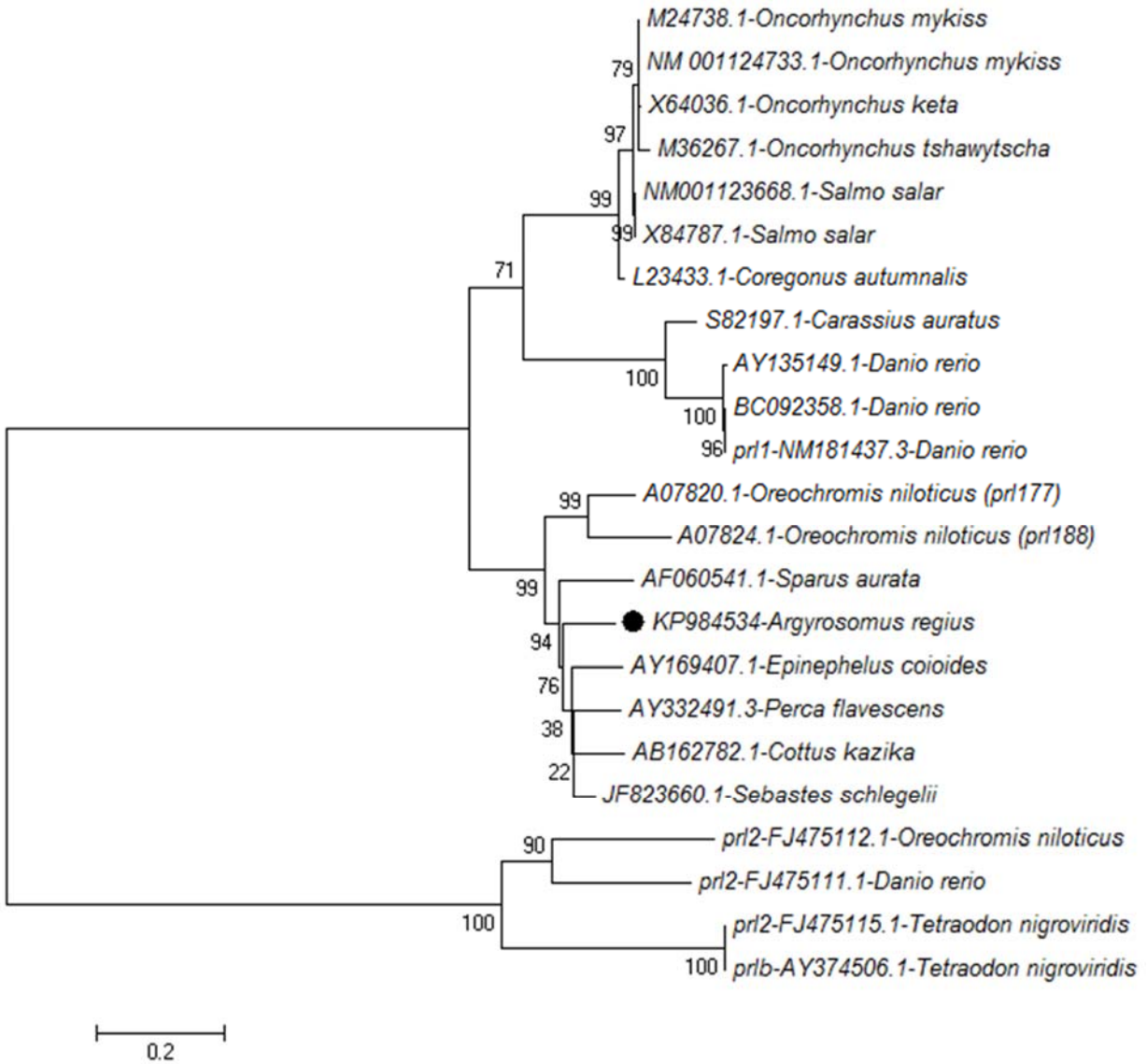
593

```
1 ctgctggagcgcgagcctctcagcgctctgacatgctgcactccctc
  L L E R A S Q R S D M L H S L
46 agcacaactctcaccaaagatctgagcaaccacgtcccacctgta
  S T T L T K D L S N H V P P V
91 ggctggacgatgatgccccgccccccattgtgccacacctcctct
  G W T M M P R P P L C H T S S
136 ctacagacacccaatgacaaggagcaagctctgcaattgtcagag
  L Q T P N D K E Q A L Q L S E
181 tcggacctgatgtcattggctcgctcactgctccaagcctggttt
  S D L M S L A R S L L Q A W F
226 gaccccctggaagtctgtccacttctgttaagaccctgcctcac
  D P L E V L S T S V K T L P H
271 ccagcccaaacagcatatccaacaagctcaaggagctgcaggag
  P A Q N S I S N K L K E L Q E
316 cactccaagagcctgggagacggcctgaacatcttatctggcaag
  H S K S L G D G L N I L S G K
361 atgggtccggcggctcagaccatctcctcactgcctacagaggt
  M G P A A Q T I S S L P Y R G
406 ggcaatgacatcggccaggataggatttccaaactgaccaacttc
  G N D I G Q D R I S K L T N F
451 catttcttggtgtcctgcttccgcccgcgactcccacaagatcgac
  H F L L S C F R R D S H K I D
496 agc498
  S
```

594

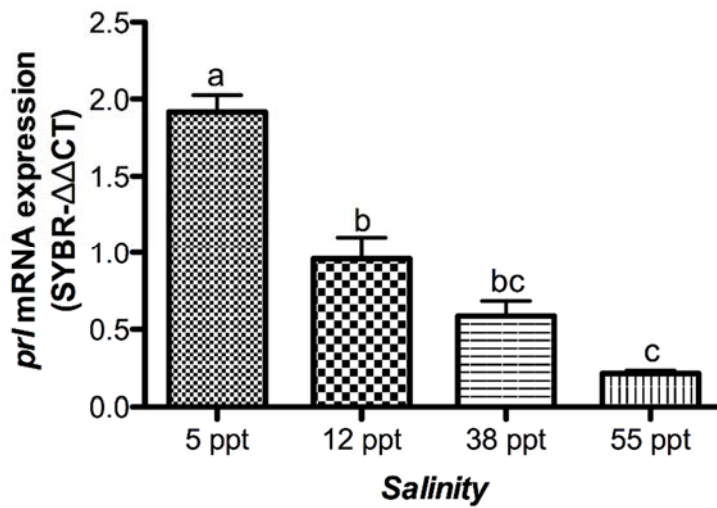
595 **Fig.1.** Nucleotide and predicted amino acid sequence of *A. regius prl* precursor.

596



597

598 **Fig. 2.** Neighbor-joining phylogenetic tree of *prl* nucleotide sequences in *A. regius*. 1,000
 599 bootstraps were used to ensure the efficacy of the test. Species and accession numbers
 600 are shown in the tree. The position of *A. regius* *prl* precursor is marked by a black circle.
 601



602
603

604 **Fig. 3.** mRNA expression patterns for *prl* in *A. regius* juveniles acclimated to different
 605 environmental salinities (5, 12, 38, and 55 ‰) during 21 days. Data are represented as
 606 mean ± standard error of the mean (SEM; n = 8). Different letters indicate significant
 607 differences among experimental groups (one way ANOVA and Tukey-HSD post-hoc, $P <$
 608 0.01).

609

```

1 ctgtcgggtggtgtctctgggtgtgtcctctcagccaatcacagac
  L S V V S L G V S S Q P I T D
46 gtccagcgtctgttctccatcgctgtgagcagagttcaacacctc
  V Q R L F S I A V S R V Q H L
91 cacctgctcgctcagagactcttctctgactttgagagctctctg
  H L L A Q R L F S D F E S S L
136 cagacggaggaacagcgtcaactcaacaaaatcttcctgcaggat
  Q T E E Q R Q L N K I F L Q D
181 ttctgcaactctgattacatcatcagtcgatcgacaagcagcag
  F C N S D Y I I S P I D K H E
226 acgcaacgcagctcagttctgaagctgctgtccatctcctatcga
  T Q R S S V L K L L S I S Y R
271 ttggtcgagtccttgggagttccccagtcgcttctctgtctggaggt
  L V E S W E F P S R S L S G G
316 tctgctccaaggaaccagatttcacccaaactttctgagctgaag
  S A P R N Q I S P K L S E L K
361 acggggatcctgctgctgatcagggccaatcaggatggagcagaa
  T G I L LL I R A N Q D G A E
406 atctttcctgatagctccgccctccagctggctccgtatgggaac
  I F P D S S A L Q L A P Y G N
451 tattatcaaagtctgagcggcgacgagtcgctgagacgaacctac
  Y Y Q S L S G D E S L R R T Y
496 gaactgctcgctgcttcaagaaagacatgcacaaggtggagacc
  E L L A C F K K D M H K V E T
541 tacctgacg549
  Y L T

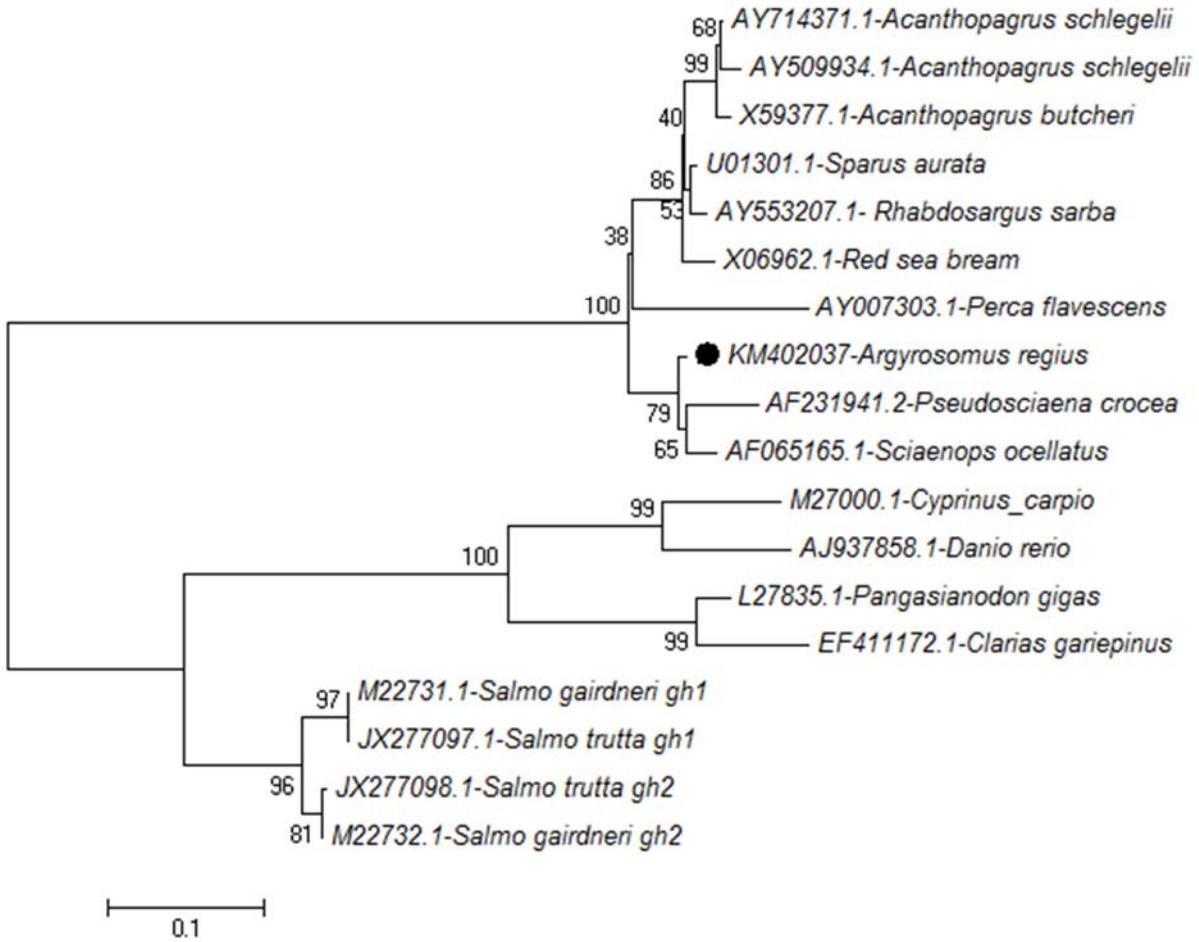
```

610

611

612 **Fig. 4.** Nucleotide and predicted amino acid sequence of *A. regius gh* precursor.

613

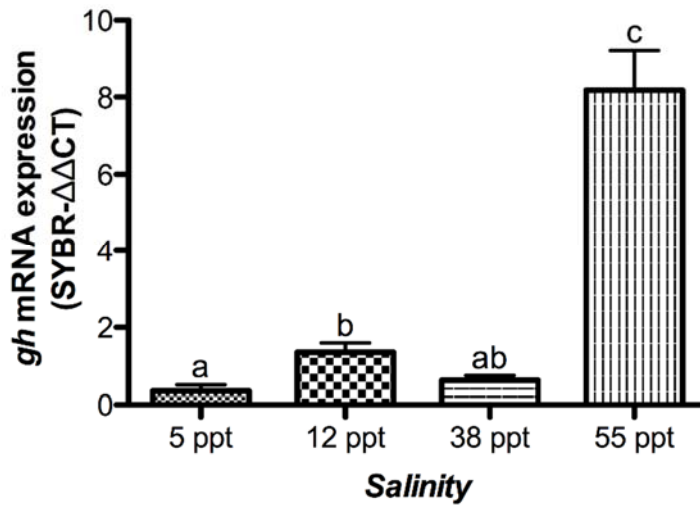


614

615

616 **Fig. 5.** Neighbor-joining phylogenetic tree of *gh* nucleotide sequences in *A. regius*. 1,000
 617 bootstraps were used to ensure the efficacy of the test. Species and accession numbers
 618 are shown in the tree. The position of *A. regius* GH precursor is marked by the black
 619 circle.

620



621

622

623 **Fig. 6.** mRNA expression patterns for *gh* in *A. regius* juveniles acclimated to different
 624 environmental salinities (5, 12, 38, and 55 ‰) during 21 days. Data are represented as
 625 mean \pm SEM ($n = 8$). Different letters indicate significant differences among experimental
 626 groups (one way ANOVA and Tukey-HSD post-hoc, $P < 0.01$).

627

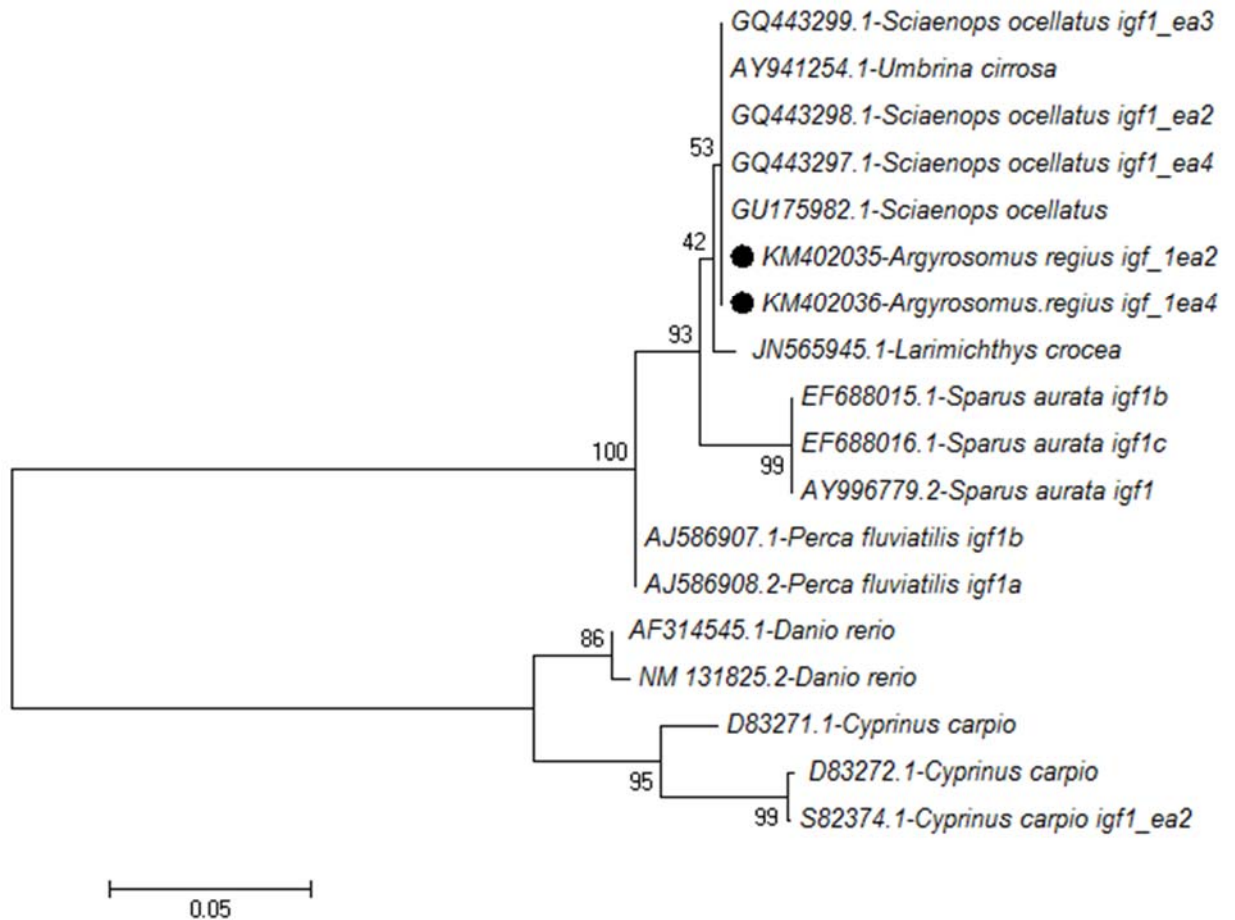
```

1   CAAGTTCATTTTCGCCCGGCTTTGTCTTGCGGAGACCCGTGGGG
45  ATGTCTAGCGCTCTTTCCTTTCAGTGGCATTATGTGATGTCTTC
    M S S A L S F Q W H L C D V F
90  AAGAGTGCATGTGCTGTATCTCCTGTAGCCACACCCTCTCACTA
    K S A M C C I S C S H T L S L
136 CTGCTGTGCGTCCCTCACCTGACTCCGACGGCAACAGGGGCGGGC
    L L C V L T L T P T A T G A G
181 CCAGAGACCCTGTGCGGGGCGGAGCTGGTCGACACGCTGCAGTTT
    P E T L C G A E L V D T L Q F
226 GTGTGTGGAGAGAGAGGGCTTTTATTTTCAGTAAACCAACAGGCTAT
    V C G E R G F Y F S K P T G Y
271 GGCCCAAATGCACGGCGGTACGCGGCATCGTGGACGAGTGCTGC
    G P N A R R S R G I V D E C C
316 TTCAAAGCTGTGAGCTGCGGCGCCTGGAGATGTACTGTGCACCT
    F Q S C E L R R L E M Y C A P
361 GCCAAGACTAGCAAGGCTGCTCGCTCTGTGCGTGCACAGCGCCAC
    A K T S K A A R S V R A Q R H
406 ACAGACATGCCAAGAGCACCTAAGGTTAGTACCGCAGGGCACAAA
    T D M P R A P K V S T A G H K
451 GTGGACAAGGGCACAGAGCGTAGGACAGCACAGCCAGACAAG
    V D K G T E R R T A Q Q P D K
496 ACAAAAAACAAGAAGAGACCTTTACCTGGACATAGTCATTCATCC
    T K N K K R P L P G H S H S S
541 TTCAAGGAAGTGCATCAGAAAAATTCAAGTCGAGGCAACACGGGG
    F K E V H Q K N S S R G N T G
586 GGCAGAAATTACCGAATGTAG
    G R N Y R M*
608 GGAAGGAGGAGGAGCGAATGGACAAATGCCAGCGACTTGGGAAG
653 AGAGAAGGGAGTGGCCTTAACTGGTA-3' UTR

```

630 **Fig. 7.** Nucleotide and predicted amino acid sequence of *A. regius igf1* precursor. As the
631 key adopted by Tiago et al. (2008) for visual description of *S. aurata* Igf1 primary protein
632 structure, Light gray box and black letters indicate the signal peptide; dark gray box and
633 black letters indicate the B domain; white box indicates the A domain; dark gray box and
634 white letters indicate the C domain; light gray box and white letters indicate the D domain;
635 and black box and white letters indicate the E domain. In the E domain, alternatively
636 spliced region present in *igf1_ea4* transcript but absent in *igf1_ea2* is double underlined
637 by white color.

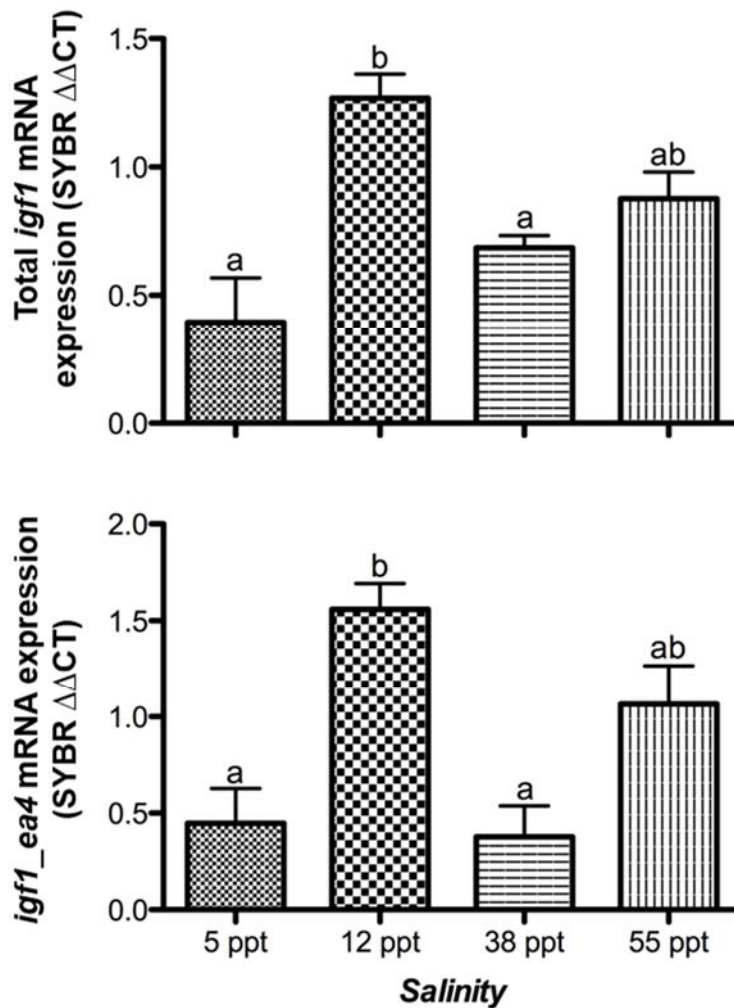
638



640

641 **Fig. 8.** Neighbor-joining phylogenetic tree of *igf1* nucleotide sequences in *A. regius*. 1,000
 642 bootstraps were used to ensure the efficacy of the test. Species and accession numbers
 643 are shown in the tree. The position of *A. regius* *igf1* precursor is marked by the black
 644 circle.

645



646
647

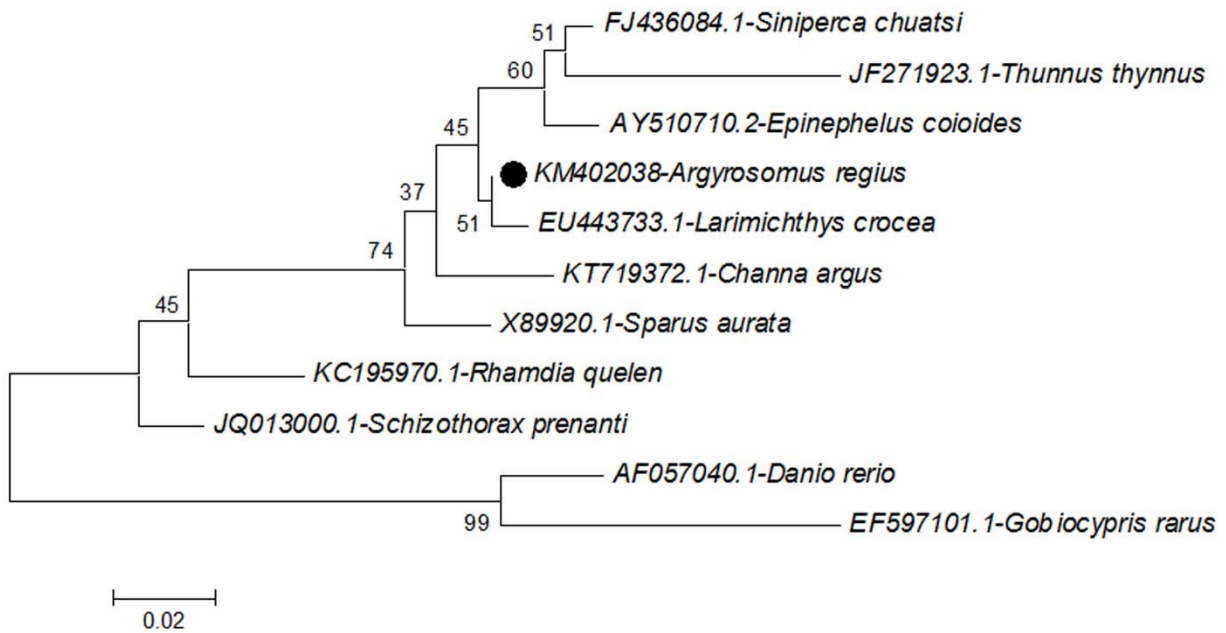
648 **Fig. 9.** mRNA expression patterns for total *igf1* transcripts (above, using primers designed
649 from the shared region in both *igf1* isoforms found) and *igf1_ea4* only (using qPCR
650 primers designed from the unique zone in isoform *igf1_ea4*) in *A. regius* juveniles
651 acclimated to different environmental salinities (5, 12, 38, and 55 ‰) during 21 days. Data
652 are represented as mean ± SEM ($n = 8$). Different letters indicate significant differences
653 among experimental groups (one way ANOVA and Tukey-HSD post-hoc, $P < 0.01$).

654

1 ATGGATGAGGAAATCGCCGCACTGGTTGTTGACAACGGATCCGGT
M D E E I A A L V V D N G S G
46 ATGTGCAAAGCCGGATTTCGCCGAGACGACGCCCTCGTGCTGTC
M C K A G F A G D D A P R A V
91 TTCCCATCCATCGTTCGGTCGCCCCAGGCATCAGGGTGTGATGGTT
F P S I V G R P R H Q G V M V
136 GGTATGGGCCAGAAGGACAGCTACGTTGGTGATGAAGCCCAGAGC
G M G Q K D S Y V G D E A Q S
181 AAGAGAGGTATCCTGACCCTGAAGTACCCCATCGAGCACGGTATT
K R G I L T L K Y P I E H G I
226 GTGACCAACTGGGATGACATGGAGAAGATCTGGCATCACACCTTC
V T N W D D M E K I W H H T F
271 TACAACGAGCTCAGAGTTGCCCTGAGGAGCACCCCGTCCTGCTC
Y N E L R V A P E E H P V L L
316 ACAGAGGCCCCCTGAACCCCAAAGCCAACAGGGAGAAGATGACC
T E A P L N P K A N R E K M T
361 CAGATCATGTTTCGAGACCTTCAACACCCCGCCATGTACGTTGCC
Q I M F E T F N T P A M Y V A
406 ATCCAGGCTGTGCTGTCCCTGTATGCCTCTGGTCGTACCACTGGT
I Q A V L S L Y A S G R T T G
451 ATCGTCATGGACTCCGGTGATGGTGTGACCCACACAGTGCCCATC
I V M D S G D G V T H T V P I
496 TACGAGGGTTACGCCCTGCCCCACGCCATCCTGCGTCTGGACTTG
Y E G Y A L P H A I L R L D L
541 GCCGGCCGCGACCTCACAGACTACCTCATGAAGATCCTGACAGAG
A G R D L T D Y L M K I L T E
586 CGTGGCTACTCCTTCACCACCACAGCCGAGAGGGAAATCGTGCGT
R G Y S F T T T A E R E I V R
631 GACATCAAGGAGAAGCTGTGCTACGTCGCCCTGGACTTCGAGCAG
D I K E K L C Y V A L D F E Q
676 GAGATGGGCACTGCTGCCTCCTCCTCCTGGAGAAGAGCTAT
E M G T A A S S S L E K S Y
721 GAGCTGCCCCGACGGACAGGTATCACCATCGGCAATGAGAGGTTC
E L P D G Q V I T I G N E R F
766 CGTTGCCAGAGGCCCTCTTCCAGCCTTCCCTCCTCGGTATGGAA
R C P E A L F Q P S F L G M E
811 TCTTGCGGAATCCACGAGACCCTACAACAGCATCATGAAGTGC
S C G I H E T T Y N S I M K C
856 GACGTCGACATCCGTAAGGACCTGTACGCCAACACCGTGCTGTCT
D V D I R K D L Y A N T V L S
901 GGAGGTACCACCATGTACCCCGGCATCGCTGACAGGATGCAGAAG
G G T T M Y P G I A D R M Q K
946 GAGATCACAGCCCTGGCCCCATCCACCATGAAGATCAAGATCATT
E I T A L A P S T M K I K I I
991 GCCCCACCTGAGCGTAAATACTCTGTCTGGATCGGAGGCTCCATC
A P P E R K Y S V W I G G S I
1036 CTGGCCTCTCTGTCCACCTTCCAGCAGATGTGGATCAGCAAGCAG
L A S L S T F Q Q M W I S K Q
1081 GAGTACGATGAGTCCGGCCCCCTCCATCGTTCAC 1113
E Y D E S G P S I V H

655

656 **Fig. 10.** Nucleotide and predicted amino acid sequence of *A. regius actb* precursor.



659

660 **Fig. 11.** Neighbor-joining phylogenetic tree of *actb* nucleotide sequences in *A. regius*.

661 1,000 bootstraps were used to ensure the efficacy of the test. Species and accession

662 numbers are shown in the tree. The position of *A. regius actb* precursor is marked by the

663 black circle.

664

665 **Tables**

666

667 **Table 1:** Sequences of primers used for cloning of the open reading frames (ORFs) of *A.*
 668 *regius prl, gh, igf1, and actb.*

669

Gene	Orientation	Sequences (5'→3')	Location in <i>A. regius</i>
<i>prl</i>	Sense	GCTGTCGGTGVTGWCTYTGG	1
	Antisense	CCGTCAGGTAGGTCTCCACC	552
<i>gh</i>	Sense	CTGCTBGABCGAGCCTCTCAG	1
	Antisense	GCTGTCRATCTTGTGVGAGTC	552
<i>igf1</i>	Sense	CAAGTTCATTTTCGCCGGGC	1
	Antisense	TACCAGKTAAGGCCACTCCC	679
<i>actb</i>	Sense	ATGGAWGABGAAATCGC	1
	Antisense	GTGRACGATGGAKGGGCC	1113

670

671

672 **Table 2.** PCR steps used for (1) cloning of *prl*, *gh*, *igf1* and *actb* intermediate fragments
 673 and (2) qPCR amplifications.

674

(1)		
Step	Temperature	Time
Initial denaturation	95 °C	10 min
40 cycles	Denaturation	95 °C 30 s
	Annealing	55 °C 30 s
	Extension	72 °C 60 s
Final Extension	72 °C	10 min
(2)		
Initial denaturation	95 °C	10 min
40 cycles	Denaturation	95 °C 15 s
	Annealing & Extension	60 °C 30 s

675

676

677 **Table 3.** Orientation, sequences, positions, GenBank accession numbers of the genes cloned and used, amplicon sizes,
 678 amplification efficiencies and regression coefficients of the primers used for qPCR amplification.

679

Primers	Orientation	Sequence 5'→3'	Position	Acc. no.	Amplicon Size (bp)	E	r ²
<i>prl</i>	Sense	TGGTTTGACCCCCTGGAA	220-320	KP984534	101	0.96	0.996
	Antisense	GAGTGCTCCTGCAGCTCCTT					
<i>gh</i>	Sense	GGAGTTCCCCAGTCGTTCTC	287-387	KM402037	101	0.99	0.99
	Antisense	CCCTGATCAGCAGCAGGAT					
<i>igf1 TOTAL</i> (<i>igf1_ea2</i> , <i>igf1_ea4</i>)	Sense	CCTTCAAGGAAGTGCATCAGA	457-556	KM402035	100	1	0.99
	Antisense	CATTTGTCCATTCGCTCCTC		KM402036			
<i>igf1_ea4</i>	Sense	GTTAGTACCGCAGGGCACAA	430-582	KM402036	153	0.99	0.99
	Antisense	CGTGTTGCCTCGACTTGAAT					
<i>actb</i>	Sense	ATCCACCATGAAGATCAAGA	966-1061	KM402038	108	1	0.99
	Antisense	GCTGGAAGGTGGACAGAGAG					

680